Implementation of Soft Computing Techniques in Forecasting Compressive Strength and Permeability of Pervious Concrete Blended with Ground Granulated Blast-furnace Slag

Boddu Sudhir Kumar[1] iD**, Kakara Srikanth[2*]** iD**, Tammali Eeshwar[3]**

1. Ph.D. Student, Department of Civil Engineering, National Institute of Technology, Warangal, Telangana, India
2. Assistant Professor, Department of Civil Engineering, GMR Institute of Technology, Rajam, Andhra Pradesh India
3. B. Tech, Department of Civil Engineering, National Institute of Technology, Tiruchirappalli, Tamil Nadu, India
Corresponding author: *srikanth.k@gmrit.edu.in*

https://doi.org/10.22115/SCCE.2023.359399.1517

ARTICLE INFO

ABSTRACT

Urban expansion and infrastructure development have exacerbated environmental issues by creating impermeable layers on the earth's surface, resulting in flash floods and reduced groundwater levels. These problems can be alleviated by using pervious concrete to enhance pavement drainage capacities. However, pervious concrete has limited applications due to its lower strength properties, which are attributed to its mix proportions featuring minimal fine aggregate quantities and an open-graded mix. This study examines the impact of incorporating Ground Granulated Blast-furnace Slag (GGBS) as a supplementary cementitious material in pervious concrete on its strength, drainage capabilities, and water absorption. Further, Artificial Neural Networks (ANN) were used to predict the mechanical and permeability properties of pervious concrete mixes with varying GGBS proportions. The study's results indicate that using GGBS as a 35% partial cement replacement with 10 mm aggregates significantly increases compressive and flexural strength by 28% and 20%, respectively. While permeability values were slightly reduced, they remained within acceptable limits for drainage properties. The developed ANN models outperformed the traditional MLR model, serving as a viable substitute logical tool for forecasting strength as well as permeability. Ultimately, adding GGBS to pervious concrete not only enhances strength but also contributes to environmentally friendly construction practices.

1. Introduction

Climate-resilient infrastructure can improve service dependability, asset durability, and economic gains in the construction sector. Concrete, a commonly used material in building construction and paving systems, offers ease of application, resistance to water and heat, and versatility in size and shape[1] . However, cement production results in significant greenhouse gas emissions, such as CO_2, exacerbating climate change. As a result, research has aimed to decrease cement consumption by partially or fully replacing it with alternative cementitious materials. Similarly, some marginal materials have been used as substitutes for natural aggregates in concrete, creating more sustainable building materials. Alternatively, pavement surfaces like roadways and streets make the earth's surface impervious, avoiding rainfall from infiltrating Intergranular micropores [2]. This leads towards "heat islands" in big cities, which release heat into the air during night time. These ecological problems stem from insufficient interaction between air, water, and soil beneath pavements [3]. Thus, it is crucial to develop climate-adaptive construction materials and execute environmentally responsive transportation infrastructure schemes to attain long lasting sustainable eco-friendly constructions. In view of sustainability, the present study is about pervious concrete containing Ground Granulated Blast-furnace Slag (GGBS) as a partial cementitious material. Porous concrete, also known as pervious or permeable concrete, is a kind of concrete that permits water to infiltrate due to its interconnected void structure. This characteristic makes it a popular choice for sustainable construction projects, as it helps manage stormwater runoff, reduces flooding, and replenishes groundwater levels. GGBS is a supplementary cementitious material (SCM) that can be used as a partial replacement for cement in concrete mixtures. GGBS is a by-product of the iron and steel industry and offers numerous environmental and economic benefits. When using GGBS as a cement replacement in pervious concrete, several advantages can be observed including: reduced CO_2 emissions, improved workability, enhanced durability, better strength development, and cost-effective [4]. On the other hand, pervious concrete controls both the quantity and quality of storm-water runoff while improving groundwater recharge conditions [5].

Pervious concrete distinguishes itself from standard concrete, through its possession of an interconnected macro-pore arrangement. This arrangement is formed by minimizing the utilization of fine aggregate, resulting in voids that facilitate the infiltration of rainwater at a velocity in the ranges of 0.19 and 0.53 cm/s [6]. Pervious Concrete Pavement (PCP) offers several benefits, including the mitigation of aquaplaning, reduction in tire-pavement interaction noise, lower energy consumption, decreased ground-water depletion, and minimized adverse effects of excess overflow and flash floods. However, the structural strength of PCP is compromised due to their high porosity, thus limiting their usage to specific areas such as parking areas, pedestrian footways, running tracks, and dedicated bicycle bays [7]. Additionally, researchers have explored the use of supplementary cementitious materials (SCMs) such as metakaolin, fly ash, GGBS, and silica fume to enhance the strength of pervious concrete pavement (PCP) and broaden its applications in medium to high traffic volume pavements. SCMs' pozzolanic capabilities allow them to react with calcium hydroxide and water in the cement matrix, resulting in improved strength [8]. These SCMs not only improve the structural and functional performance of the pavement but also provide environmental benefits by reducing

waste disposal issues, conserving natural resources, and lowering carbon emissions. Generally, SCMs influence concrete properties through two primary reactions. The first reaction, hydration, occurs when SCMs react with water and calcium hydrate to produce C-S-H gel, alike cement hydration. The second reaction involves biochemical reactivity, where SCMs interact with hardened cement and moisture, forming a secondary structural layer that densifies the fine-texture [8]. It is worth noting that the ideal amount of GGBS replacement in pervious concrete is determined by a number of criteria, including desired performance, local availability, and cost. Common replacement levels range from 20% to 70%, but it is essential to conduct proper mix design and testing to determine the appropriate level for a specific application [9]. As a byproduct of the steel industry, GGBS has been utilised as a partial cement alternative to reduce carbon footprints and enhance surface finishing in ordinary concrete [10]. However, the integration of GGBS in pervious concrete has received little attention, despite the fact that concrete containing 75% GGBS is more impermeable than Portland Pozzolana Cement concrete [11]. Nonetheless, GGBS has the potential to strengthen porous concrete when utilized in lesser proportions (less than 65 %) [12]. In 2018, research was undertaken to investigate the strength and permeability properties of porous concrete when 50% cement was replaced with GGBS [13]. Their findings suggest to use GGBS as a substitute for OPC results in a more sustainable material by reducing construction costs, climate change impact, and emissions. The study also observed a 54% decrease in carbon emissions.

The development of mathematical models is crucial in predicting the properties of pervious concrete. Models of this type allow for thorough analysis, hypothesis formulation, and event prediction. Developing an accurate mathematical model, on the other hand, is a difficult undertaking that necessitates knowledge in both mathematics and engineering. Numerous studies have been conducted worldwide to develop models for predicting the properties of conventional concrete. For instance, Almasaeid and Salman (2022) [14], developed an Artificial Neural Network (ANN) model based on feedforward backpropagation. The results demonstrated that the ANN model outperformed regression analysis in predicting the properties of permeable concrete. In another study, Adewumi et al. (2016) [15] used support vector regression (SVR) to estimate the physical, mechanical, and hydrological properties of pervious concrete. Their computational intelligence approach displayed remarkable generalisation and prediction capabilities, demonstrating the potential for improving the performance of previous concrete. However, there has been little study into forecasting the characteristics of pervious concrete including SCMs, and no studies have been undertaken to construct a prediction model for GGBS-incorporated pervious concrete utilising soft computing approaches.

Artificial Neural Networks (ANN) are computational models based on the neural structure of the human brain that can learn from input and recognise complicated patterns [16]. Due to the ability of accurately prediction, ANNs have been used in number of complex problems like air quality prediction [17], SARS-CoV-2 transmission probability [18], CO_2 content prediction [19]. Similarly, various researchers have employed ANN for the prediction of different concrete properties. Apart from conventional properties the ANN have been used for special concretes like concrete with fly ash [20], Fiber Reinforced Plastic (FRP) reinforced concrete [21], corroded

reinforced concrete beams [22], and other types of concrete. The researchers employed an ANN for forecasting the strength of porous concrete containing silica fume. By working out a subsection of the data points with input parameters from the constituent materials, the ANN emerged as the most effective technique for predicting compressive strength. Similarly, another study examined the effects of volcanic ash as an SCM on the accomplishment of porous concrete [23]. The researchers created 21 concrete mixes with varying water-cement proportions (0.55, 0.65, and 0.75) and SCM ratios (0, 15%, 25%, and 30%). An ANN prediction model was created using a feed-forward and back-propagation network to examine water penetration, penetrability, and strength. The findings showed that the ANN was accurate in capturing the effect of input factors on the desired output. ANNs may be used to forecast compressive strength and permeability in the context of pervious concrete with GGBS, which are critical criteria for evaluating the performance of this sustainable building material [24]. By using historical and experimental data on different mix proportions, GGBS replacement levels, aggregate sizes, and curing times, an ANN model can be trained to recognize the relationships between these factors and the resulting compressive strength and drainage characteristics of porous concrete. The trained model can then be used to make accurate predictions for new mix designs, saving time and resources by reducing the need for extensive laboratory testing. This application of ANN in pervious concrete with GGBS facilitates optimization of mix proportions, ensuring the desired strength and permeability characteristics are achieved while maintaining environmental benefits. As a result, the construction industry can make more informed decisions in designing and implementing pervious concrete pavements, particularly in high or mid-volume roads where strength and drainage properties are vital.

The authors erstwhile published research article on usage of high-volume SCMs in PC, elaborates on the mechanical and hydrological properties of PC [25]. The studies major hypothesis is about the role of SCMs in PC at a high-volume cement replacement. Unreacted SCMs are seen to operate as fine aggregate during a high-volume replacement of SCMs, and this has a major influence on the characteristics of PC. There have been few investigations on the characteristics of PC with high volume SCMs. As a result, the current research intends to forecast the compressive strength and permeability of PC using ANNs. For this purpose, the two independent variables are determined at various mix proportions using the experimental studies and then ANN models are developed for the same. Furthermore, the ANN models created are compared to models developed using multiple linear regression analysis.

2. Research background

2.1. Artificial neural networks

Analogous to the acquisition of novel abilities by a newborn through iterative training, ANNs necessitate training to execute designated tasks. ANNs exhibit parallelisms with the human nervous system, processing extensive datasets to generate intended outputs. Consequently, they provide instantaneous resolutions and alternative methodologies for intricate predicaments that

prove demanding for alternative technological solutions [26]. ANNs consist of five basic structural components: the input layer, which provides information to the network; weights, which are variables that control the impact of input signals; the summation function; the activation function; and output function. The activation function of a neuron determines its activation status, deciding whether it should be active or inactive [27]. The sigmoid activation function which is most commonly utilized, can be seen in Equation 1:

$$(outcome) = \frac{1}{1+e^{-\alpha(sum)}} \tag{1}$$

Here, α denotes a constant employed to alter the slope of the function. ANNs receive input, organize them in the form of patterns, and forecast outputs for alike data points. The neural structure encompasses an input component, a computational hidden layer, and an output component responsible for forecasting the actual outcomes.

The artificial neural network (ANN) comprises an input layer, where each neuron represents a discretized state of the system at a given time. This input layer is linked to a single hidden layer, which is connected to the output layer. The interconnections between the layers are realized by nodes, with the strength of their connections quantified by numerical values as shown in Figure 1. The node is shown as a circle with two sections: the summing function on the left and the activation function on the right. X_1, X_2 and X_3 are the input signals and w_1, w_2 and w_3 are the corresponding weights of the three input signals. When inputs (i.e., $\Sigma x_i w_i$) enter the node, the summing function computes their weighted sum. The activation function decides whether or not to activate the neuron and creates an output based on the input. As the activation function, the sigmoid (logistic) function is widely utilised. A neural network may be taught to recognise patterns and correlations in input data by making repeated weight modifications. The ANN receives input and output data from a training dataset throughout the training phase, adjusts link weights, and minimises the difference between anticipated and goal values. This method is continued until the performance criterion is reached throughout numerous training cycles, or epochs. In this study, the ANN model was built using the MATLAB Neural Network Toolbox. [28,29]. This approach provides a means of developing a neural network capable of identifying patterns and relationships within input data.
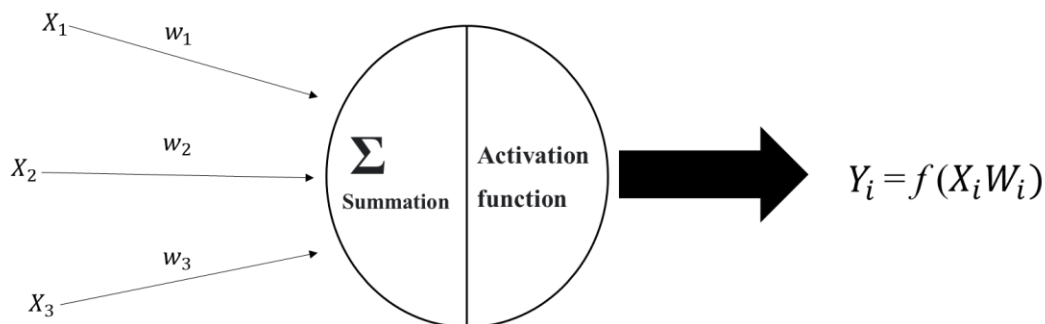
Fig. 1. The schematic approach of the ANN model.

The mean square error (MSE) between the predicted output and the target output for a particular sample size was used to evaluate the neural network's performance in this study. To compute the MSE, the output vector from the neural network was compared with the targeted output vector, and the error vector was calculated for the output layer neurons. If the MSE is less than the desired error (goal), the training of the neural network is considered complete, and the network is ready for prediction. Otherwise, the weights are updated until the desired error goal is achieved. The effectiveness of the neural network training largely depends on the learning algorithm used to obtain better memorization and generalization capability. In this study, the Levenberg–Marquardt (L–M) algorithm was employed to update the weights in the proposed ANN model. Once the training is completed, the predictive capability of the network is tested on unknown input data to verify its accuracy. A multilayer feed forward network, as shown in Figure 2 has input vector (x_i) and corresponding target output vector (o_i) with hidden layers as (h_i).
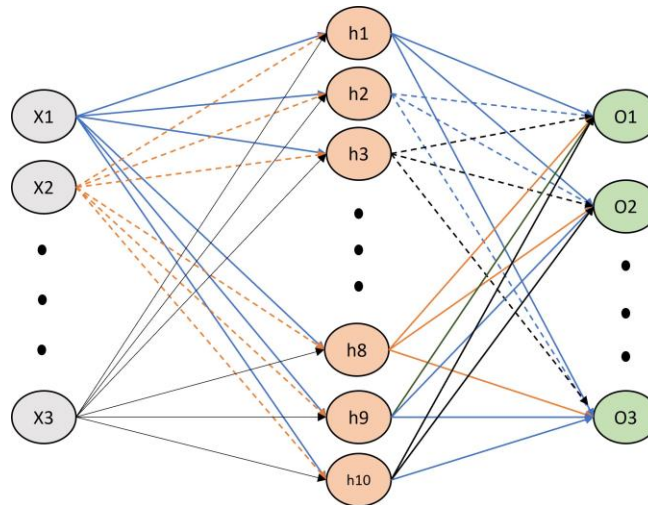

Fig. 2. Multilayer feed forward network.

3. Methodology

3.1. Materials

For PC samples production, Ordinary Portland Cement (OPC) of Grade 43 is used as the primary binder material. This cement complies with the IS: 4031 – 1996 [30] standard, ensuring its quality and suitability for various construction applications. Grade 43 OPC indicates that the cement has a minimum compressive strength of 43 MPa after 28 days of curing, making it ideal for structural elements, including pervious concrete. Further, crushed gravel was used as coarse aggregate, available in two size ranges: 4.75 to 9.5 mm and 9.5 to 19 mm. The gradation in two size ranges is shown in Figure 3. These aggregate sizes were chosen to provide a well-graded particle distribution, ensuring a suitable pore structure and mechanical performance for the pervious concrete mix. The aggregates were sourced from a local quarry, where they were processed and crushed to obtain the desired size ranges. The selected aggregates were of high quality, being hard, clean, free of surface coatings, and devoid of any fissures that might

compromise the concrete's performance. Before being incorporated into the pervious concrete mix, the aggregates underwent a cleaning and drying process. First, they were washed thoroughly to remove any dust, dirt, or organic materials that could negatively affect the bond between the cementitious matrix and the aggregates. After washing, the aggregates were air-dried in the sun for three days to eliminate any surface moisture. Following the air-drying process, the aggregates were dried in oven for one complete day and night at a temperature of 115 ± 5 °C. This step ensured complete removal of moisture from the aggregates, as excessive moisture can impact the concrete's workability, water-to-cement ratio, and ultimately, its mechanical properties. With clean and dry aggregates, the study could effectively evaluate the impact of GGBS as a partial cement replacement on the pervious concrete's performance. The physical properties of the aggregate tested in the present study are shown in Table 1.
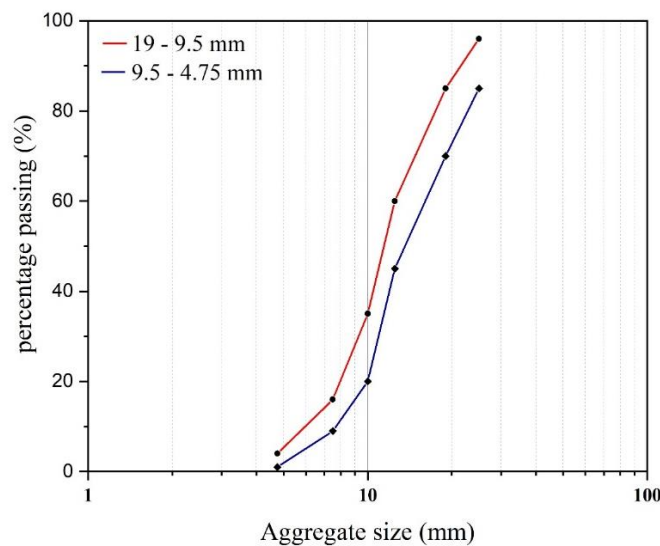
Fig. 3. Particle size distribution of coarse aggregates.

Table 1
Physical properties of the aggregates.

| Property	Observed value	Requirement as per IS: 383
Type of aggregate	Natural granite	
Aggregate Crushing value	15 %	Should be less than 45%
Aggregate Impact value	18%	Should be less than 45%
Aggregate Abrasion value	20%	Should be less than 30%
Water absorption	0.7%	Should be less than 2%
Fineness Modulus	6.7	More than 6.0 and less than 6.9
Specific gravity	2.9	More than 2.5 and less than 3.0

GGBS is generated during the process of quenching molten iron slag from a blast furnace in water or steam. In this study, GGBS was taken from a manufacturing agency, ensuring an eco-friendly and sustainable utilization of the waste material. Table 2 displays the chemical configuration of cement and GGBS accompanied by their respective physical features. GGBS

was used as a partial replacement for cement in proportions of 20%, 35%, and 50%. These percentages were chosen to investigate the optimal replacement level to improve the pervious concrete's mechanical properties and environmental benefits while maintaining its workability and durability. Before incorporating GGBS into the concrete mix, it underwent a drying process to reduce the moisture content. Initially, the GGBS sample was sun-dried for three days, which helped evaporate most of the surface moisture. Following this, the sample was dried in oven for one complete day and night at a temperature of 115 ± 5 °C, ensuring the complete removal of wetness. This step was crucial, as excessive moisture in GGBS could impact the water-to-cementitious material ratio and, consequently, the mechanical properties and performance of the pervious concrete. With a properly dried GGBS, the study could effectively evaluate its influence as a partial cement replacement on the compressive strength, permeability, and flexural strength of pervious concrete. Figure 4, illustrates the methodology adopted in the study.

Table 2
Chemical composition and physical properties of cement and GGBS.

| Material | Chemical composition (%) | | | | | | | | Physical properties | |
	SiO_2 Silicon dioxide	Al_2O_3 Aluminum Oxide	Fe_2O_3 Hematite	CaO Calcium oxide	MgO Magnesium oxide	SO_3 Sulphur trioxide	K_2O Potassium oxide	Na_2O Sodium oxide	Specific gravity	Surface area (m^2/kg)
Cement	22.3	4.4	1.9	63.4	1.7	3.8	0.8	0.18	3.15	335
GGBS	34.6	10.7	0.5	41.9	8.2	0.4	3.25	-	2.79	610
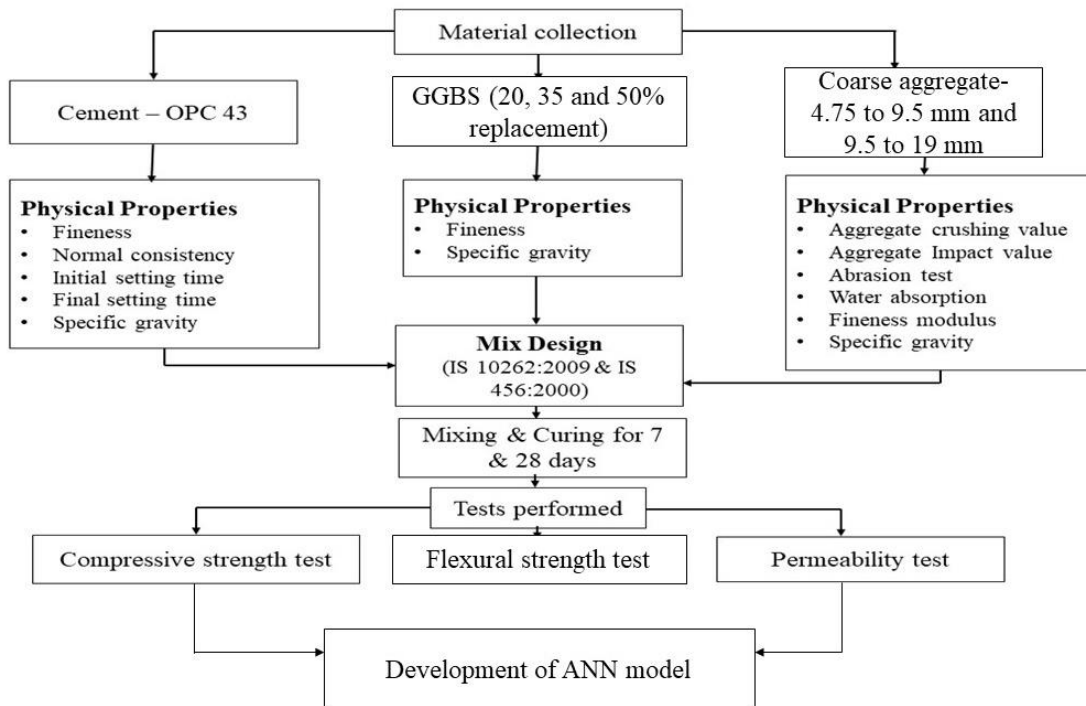
Fig. 4. Methodology of the research.

3.2. Mix design

Unlike conventional concrete, the mix design of PC is unique. Along with the compressive strength, the permeability is an important design factor for PC. The desired permeability is achieved by adopting a no fines mix for the concrete. The mix design procedure adopted in the study is based on the guidelines IRC: 44 (2017) [31]. The design procedure is for M20 mix, thus the target strength for the PC mix is 26.6 N/mm^2. The guidelines recommend a voids ratio of 15% for the desired permeability. Thus, based on the relative volume of aggregates and the volume of voids, the cement paste required for the bond between the aggregates is determined. Initially for the desired target strength, the Water to Cement (W/C) is fixed, and from which the quantity of water and cement for 1 m^3 of PC is fixed. Three replacement percentages (20%, 35%, and 50%) of GGBS by the weight of cement are used in the PC mix. The study involves 18 different PC mixtures with varying constituents. Table 3 displays the adopted designations, respective constituents in each PC mix, and the quantities of each ingredient required to produce one cubic meter of the PC mixture.

3.3. Sample preparation

The samples preparation for compressive strength, permeability, and flexural strength testing involves various steps. The first step is thoroughly mixing the cement, GGBS, coarse aggregates, and water in the desired proportions according to the mix design. The constituents are well combined to achieve a homogeneous mixture. For compressive strength testing, the mixture is casted in standard cube moulds, typically 150 mm x 150 mm x 150 mm. For flexural strength testing, the mixture casted in beam moulds, of size 150 mm x 150 mm x 500 mm. For permeability testing, the mixture is casted in cylindrical molds, of 100 mm in diameter and 200 mm in height. After placing the mixture in the moulds, the air bubbles or voids are removed by tapping the sides and by compaction. After casting, samples are covered with a plastic sheet to prevent moisture loss and allow them to set for 24 hours at room temperature. Once the initial setting is completed, the samples are removed from their molds and placed them in a curing tank filled with water for a specified curing period, typically 28 days. The curing water temperature is maintained at a temperature of 27 ± 2 °C. After the curing period, the samples are removed from the curing tank and dried for a short time to remove excess surface moisture. For compressive strength testing, the cube samples were placed in a compression testing machine and applied load until failure. For flexural strength testing, the beam samples were placed in a flexural testing machine and applied the load at the center of the beam until failure. For permeability testing, a suitable permeability apparatus, constant head permeameter is used to determine the coefficient of permeability of the cylindrical samples. The sample preparation and testing are shown in the Figure 5. The results of each test are recorded and the compressive strength, flexural strength, and permeability of the samples is calculated. The data is further analyzed to determine the performance of the pervious concrete with GGBS and its suitability for the intended applications.

Table 3
Proportions of various constituents in 1 m^3 of pervious concrete blended with GGBS.

Specimen	Aggregate (kg)		Cement and SCM (kg)		Water (kg)	$\dfrac{Water}{Cement}$	Void space (%)	Density (kg/m^3)
	10 mm	20 mm	OPC	GGBS				
Mix20-10-10	1237	-	448	109	151	0.3	10	1948
Mix20-10-15	1219	-	439	110	151	0.3	15	1930
Mix20-10-20	1210	-	431	111	151	0.3	20	1909
Mix20-20-10	-	1249	472	122	151	0.3	10	1981
Mix20-20-15	-	1219	464	120	151	0.3	15	1950
Mix20-20-20	-	1209	457	109	151	0.3	20	1945
Mix35-10-10	1048	-	398	100	151	0.3	10	1702
Mix35-10-15	1013	-	390	95	151	0.3	15	1660
Mix35-10-20	976	-	379	90	151	0.3	20	1609
Mix35-20-10	-	1064	409	108	151	0.3	10	1731
Mix35-20-15	-	1030	411	109	151	0.3	15	1682
Mix35-20-20	-	990	399	100	151	0.3	20	1609
Mix50-10-10	950	-	360	90	151	0.3	10	1539
Mix50-10-15	796	-	350	85	151	0.3	15	1390
Mix50-10-20	689	-	339	81	151	0.3	20	1290
Mix50-20-10	-	971	380	109	151	0.3	10	1569
Mix50-20-15	-	806	369	99	151	0.3	15	1408
Mix50-20-20	-	710	359	91	151	0.3	20	1320

**Fig. 5.** Pervious concrete mix, sample preparation, curing and testing involved in the study

3.4. Mechanical testing

To conduct the compressive strength testing procedure for pervious concrete (PC) with GGBS, the guidelines laid in IS: 516 (1959) [32] are followed. Upon completing the curing period, the samples are removed from the curing tank and allowed them to dry for a short time to remove excess surface moisture. The dried cube samples are placed between the plates of a compression testing machine, ensuring they are properly aligned. Gradually the load is applied at a uniform rate until the sample fails. The maximum load at which the sample fails is recorded. The maximum load is divided by the cross-sectional area of the cube to obtain the compressive strength. At a specific mix proportion, the average compressive strength of three samples is reported as the compressive strength.

The flexural strength testing procedure for PC is done as per the specifications of IS: 5816-1999 [33]. Figure 6 shows the testing setup for flexural strength testing. The dried beam specimen is placed on a flexural testing machine, which supports the specimen at two points, typically at one-third of the span length from each end. A concentrated load is applied at the center of the specimen, dividing the span length into equal thirds. The load is gradually increased at a uniform rate until the specimen fails. The maximum load at which the specimen fails is recorded and the flexural strength (f_b) is calculated using the Equation 2.

$$f_b = \frac{pl}{bd^2} \text{ (when a > 13 cm for 10 cm specimen) or } f_b = \frac{3pl}{bd^2} \text{ (when 11< a < 13 cm for 10 cm specimen)} \qquad (2)$$

Where a is the distance between the line of fracture and the nearest support, b is the width of the specimen (cm), d is the failure point depth (cm), l is supported length (cm), and P is the maximum load (Kg).
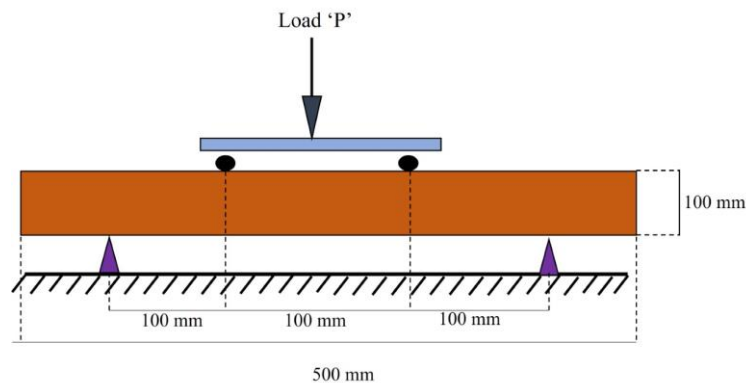
Fig. 6. Schematic representation of three-point load system for flexural strength test.

3.5. Permeability test

The constant head permeability test is conducted to determine the coefficient of permeability (k) of pervious concrete with GGBS. The test procedure followed is as per guidelines of ACI 522R-10 [34]. The sample for constant head permeability is prepared with PVC pipes as mould. The PC mix is filled and compacted to avoid air bubbles or voids. After the curing period, the test

setup is prepared using a permeability testing apparatus. The cylindrical specimen is placed horizontally in the test chamber and ensured it is properly sealed to prevent sidewall leakage. A constant head of water is established in the system by maintaining a constant water level above the specimen. The test is started by allowing water to flow through the specimen. The volume of water discharged (Q) and the time (t) it takes for the water to pass through the specimen is measured in the test. The determination of the permeability coefficient (k) involves the utilization of the mathematical expression provided in Equation 3. The visual depiction of the experimental arrangement for the constant head permeability test can be observed in Figure 7.

$$k = \frac{Q*L}{A*h*t} \tag{3}$$

Here, k is the permeability coefficient, "Q" is discharge (cm^3), "L" is the height of the sample (cm), "A" is the area of the sample (cm^2), "h" is the water height (cm), and "t" is time (sec).
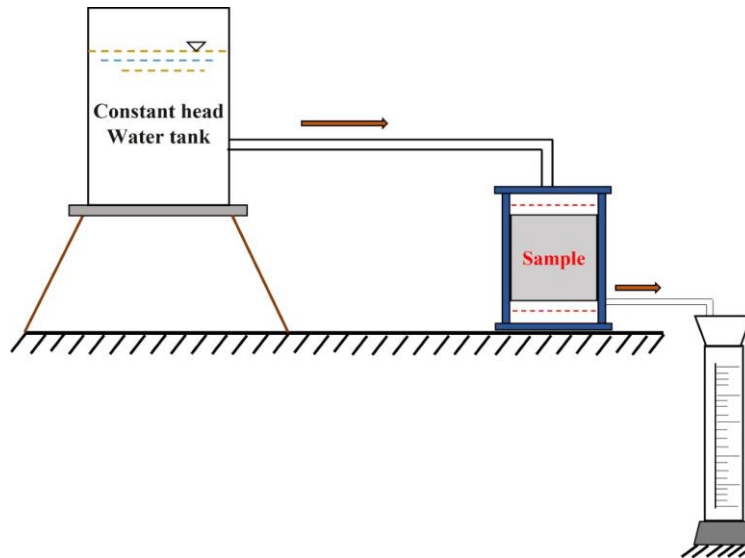

Fig. 7. Illustration of the experimental procedure for constant head test.

3.6. Water absorption

The water absorption test is employed to assess the water tightness of concrete specimens by measuring the volume of water absorbed while submerged. Pervious concrete cubes are submerged in water for 7 and 28 days, then removed from the curing tank and oven-dried at 100 °C. The weight of the dried concrete is recorded as the dry weight (W_1). Subsequently, the specimen is submerged in water, and its weight is noted as (W_2). To prevent water from flowing out, the specimen's peripheral surface is adequately covered with a non-absorbent material for a specific duration. The water absorption is calculated using the given Equation 4.

$$Water\ absorption\ (\%) = \frac{W2-W1}{W1} \times 100 \tag{4}$$

3.7. ANN Architecture

Artificial Neural Networks (ANN) establish complex non-linear relationships between dependent and independent variables. Although a trained neural network can compute outputs based on input sets, it can be challenging to find the relations among input variables and output variables. Determining the over-all input component, a computational hidden layer, and an output component is essential. The entire structure typically contains of at least 3 layers: one input layer, one or two hidden layers, and output component. In this research, two ANN structures were established: ANN_1 for predicting strength and ANN_2 for water penetrability. The entire system created in this study includes:

- The input layer consists of four neurons ($N_i = 4$), where each neuron represents distinct variables, including the amount of cement (kg), the amount of GGBS (kg), the size of the aggregate (mm), and the porosity of the material (%).
- A hidden component layer with eight or twelve neurons in ANN_1 and ANN_2.
- The neural network architecture consists of a solitary neuron within the output layer, which is dedicated to predicting the values of compressive strength (measured in MPa) and water permeability (measured in cm/s).

This study uses MATLAB to develop the structure of the network, as illustrated in Figure 8 and 9. Levenberg-Marquardt back-propagation serves as the training function, while the hyperbolic tangent sigmoid functions as the transfer function. In relation to network performance, the computation of the training rate was conducted to assess the adaptation of connection weights during the training process. To attain the most favorable performance outcomes, the training rate and momentum were adjusted for each artificial neural network (ANN). The dataset was partitioned into three distinct subgroups, where 75 % of the data was allocated for training, 15 % for testing, and the remaining 10 % for validation purposes.

In order to validate the performance of the developed ANN_1 and ANN_2, three criteria were assumed:

i. The Root Mean Square Error (RMSE), defined by Equation 5, is employed to evaluate the error measurements encountered during the three phases of Artificial Neural Network (ANN) models [34].

$$Root\ Mean\ Square\ Error = \sqrt{\frac{\sum_1^n (E-F)^2}{n}} \tag{5}$$

Where, "E" is the experimented value, "F" is the forecasted value, and n is the sample size.

ii. The Mean Absolute Percentage Error (MAPE), represented by Equation 6, is employed to compute the average of the absolute percentage discrepancy [35].

$$Mean\ Absolute\ Percentage\ Error = \frac{\sum_1^n \left|\frac{E-F}{E}\right|}{n} \times 100 \tag{6}$$

iii.   The R-square, coefficient of determination quantifies the total proportion of variation in a model, expressing it as a percentage. It is calculated using Equation 7 [36], which serves as a means to ascertain the value of R^2.

$$R^2 = 1 - \frac{square\ of\ residuals}{square\ of\ predicted\ values} \tag{7}$$
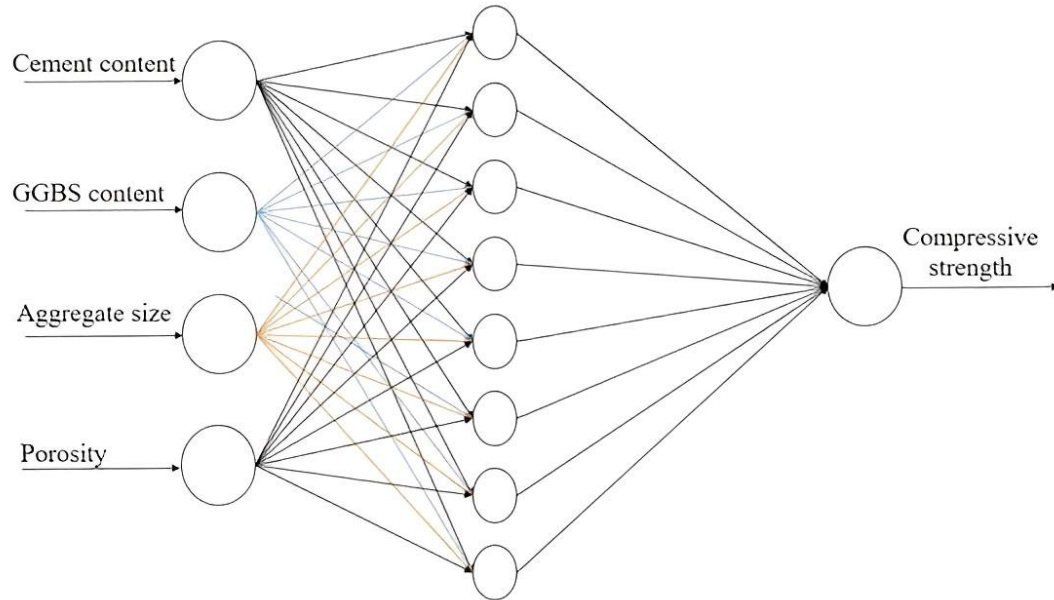
Fig. 8. ANN_1 architecture was employed to forecast the compressive strength.
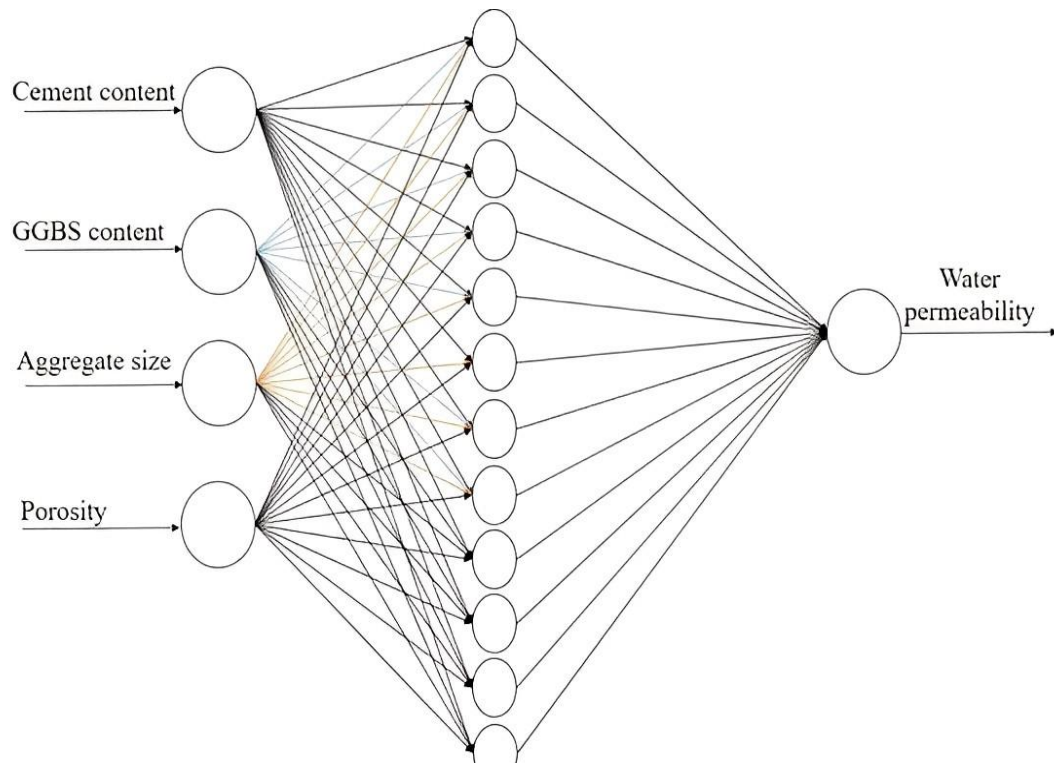
Fig. 9. ANN_2 architecture was employed to forecast permeability.

4. Results and discussion

4.1. Compressive strength

Figure 10 presents the compressive strength at 7 and 28 days for various pervious concrete samples containing GGBS. The study found that, compared to the standard mix at different curing periods, compressive strength increased with GGBS replacement levels. However, the increase occurs from 20 to 35% and then decreases from 35 to 50%. The compressive strength of conventional pervious concrete after 7 days of curing is 10.5 MPa, and it was observed that adding GGBS to cement at levels of 20%, 35%, and 50% resulted in compressive strength increases of 9.5%, 25.3%, and 8.5%, respectively. Likewise, conventional pervious concrete exhibited a compressive strength of 12.8 MPa after 28 days of curing. Similar compressive strength increases of 10.5%, 28.6%, and 8.8% were observed for 20%, 35%, and 50% GGBS replacements, respectively. The results consistently show an increase in compressive strength with GGBS levels up to 35% during all curing stages, with a decline in strength beyond that point. Experimental research on standard pervious concrete reported analogous findings, with Siddique and Kadri (2011) and Wild et al. (1996) [35,36] demonstrating that GGBS replacements for cement led to compressive strength increases of approximately 12 to 25%, which subsequently decreased once the optimum strength was reached.

The strength enhancement due to GGBS addition to pervious concrete could be attributed to its high pozzolanic reactivity. A close examination of GGBS and cement's chemical composition reveals that the high percentage of silicon dioxide (SiO_2) and aluminum oxide (Al_2O_3) in GGBS reacts with the calcium hydroxide ($Ca(OH)_2$) in cement to form a gel-like substance called C-S-H gel. This gel's strength increases with higher GGBS replacement levels. However, as the GGBS proportion further increases, aggregate interlocking becomes more dominant, resisting further compaction and counteracting the effect of GGBS replacement. As a result, the C-S-H gel's strength decreases due to aggregate packing. This effect is evident in the concrete specimens' density, where an increasing trend occurs from 20 to 35% GGBS replacement, and a significant density reduction happens at 50% replacement due to aggregate interlocking domination. When 10 mm aggregates were used instead of 20 mm aggregates, the concrete specimen's density was higher. This observation suggests that the optimal compressive strength for GGBS in pervious concrete can be achieved with a 35% replacement level and a 10 mm aggregate size.

Additionally, the pervious concrete samples were examined using Scanning Electron Microscope (SEM) images. As depicted in Figure 10, SEM images display a denser microstructure in the mixtures with increased GGBS replacement levels of 35% and 50%. The circular sections represent voids, while the white layer corresponds to the C-S-H gel. In Figure 11(a), the formation of the C-S-H gel is clearly visible, indicating a stronger bond strength. However, in Figure 11(b), the C-S-H bond is disrupted due to enlarged pore size, which weakens the bond strength. To study the impact of the size of aggregate for the specimen designated as Mix20-10-10 and Mix20-20-10, Mix350-10-10 and Mix35-20-10, and so on, were evaluated. The research Zhong & Wille (2016) concludes that, an open grade mix with larger aggregates induces higher

porosity [37]. Hence, in order to uphold a consistent porosity of 10% while utilizing 20 mm aggregates, an augmented amount of cementitious substance was incorporated in contrast to mixtures encompassing 10 mm aggregates. Thus, it is discernible that large sized aggregates and amplified cementitious materials play a role in augmenting compressive strengths.
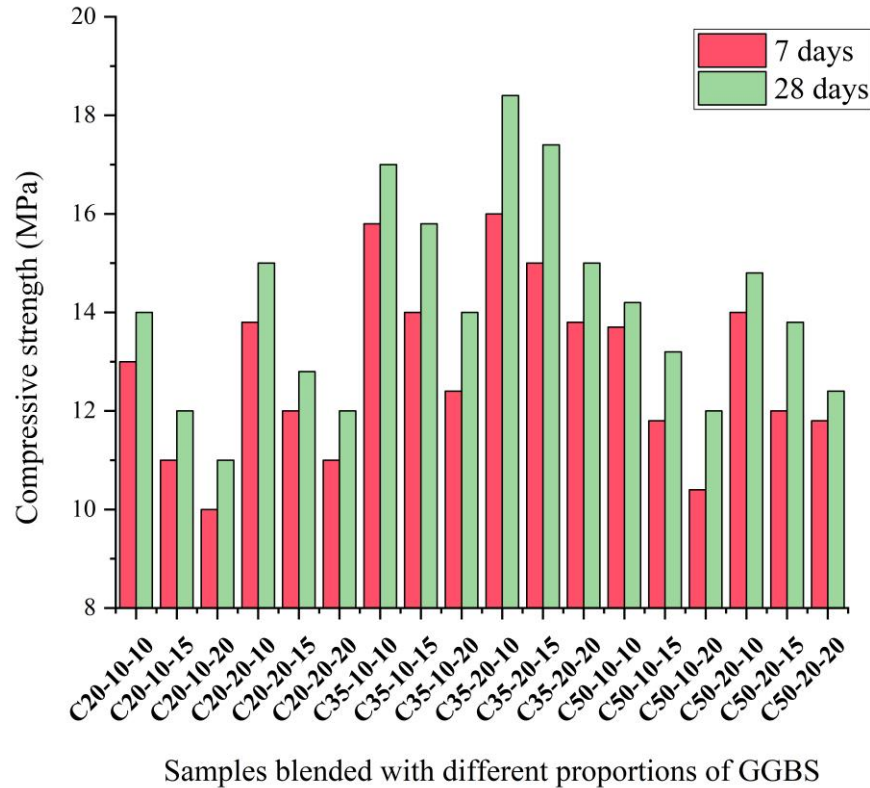
Fig. 10. Compressive strength variation for 7-days and 28-day curing of pervious concrete mixes

(a)   (b)
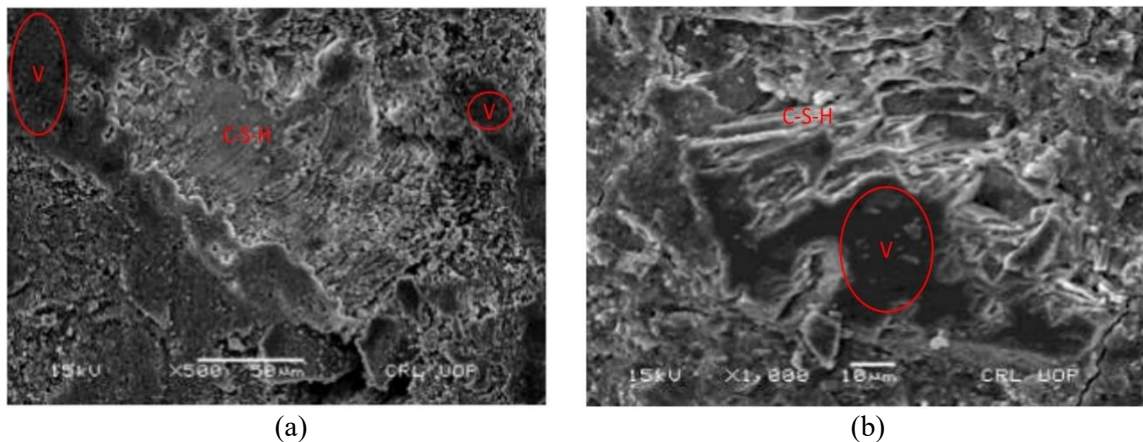
**Fig. 11.** SEM micrographs of porous concrete mix with (a) 35% replacement of GGBS, and (b) 50% GGBS replacement.

4.2. Flexural strength

Figure 12 shows the changes in flexural strength for different GGBS proportions. This variation exhibits a pattern at 28 days of curing that is similar to compressive strength. However, at 7 days

of curing, the trend appears to be in the opposite direction. Flexural strength decreased after 7 days of curing when GGBS replacement increased from 20% to 50%. Conventional pervious concrete has a flexural strength of 1.85 MPa after 7 days of curing, and it was observed that incorporating GGBS with cement at levels of 20%, 35%, and 50% led to a 9.5%, 7.3%, and 12.4% decrease in compressive strength, respectively. In contrast to the results after a 7-day cure, a 28-day cure demonstrated an increasing trend. Compared to the conventional pervious concrete's 2.1 MPa flexural strength, increases of 11.5%, 20.2%, and 9.3% were noted with GGBS replacing cement at 20%, 35%, and 50%, respectively. The decline in flexural strength after 7 days of curing was due to the low pozzolanic activity of GGBS at an early age, but after 28 days of curing, the influence of pozzolanic activity was evident as the strength increased.

As a result, the flexural strength closely matches with compressive strength, showing that at 20%, there is a modest gain in strength, at 35%, strength improves noticeably, and at 50%, strength decreases. Thus, it suggests that 35% of GGBS is the optimum dosage of cement replacement in pervious concrete. The optimum dosage of replacement would result in pervious concrete pavements with increased compressive and flexural strength. Compressive strength and flexural strength are the most important characteristics of concrete pavement construction. A replacement percentage of 35% increases the compressive strength by 20 to 25% and flexural strength by 15 to 20%. As per ACI 522 R [34], a compressive strength in the range of 2.5 to 25 MPa is desired. Similarly, a flexural strength of 0.5 to 4.8 MPa, and porosity in the range 10 to 20% is desired.
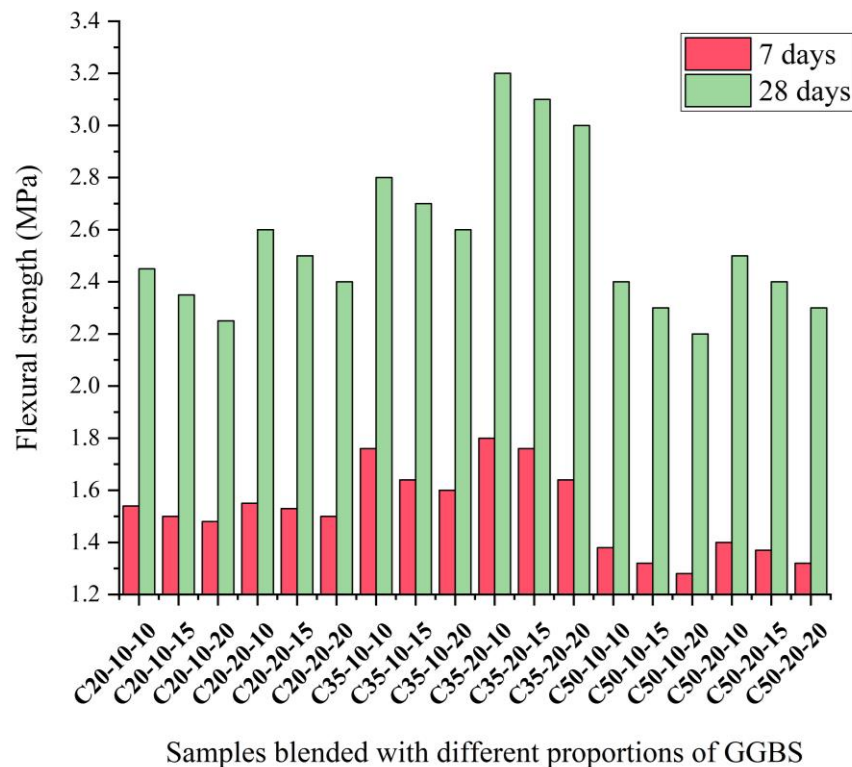

Fig. 12. Flexural strength variation for 7-days and 28-day curing of pervious concrete mixes.

4.3. Permeability

A constant head permeability test is applied to analyze the effects of porosity, and Figure 13 illustrates the permeability coefficient (k). The findings indicate that as the porosity of pervious concrete increases, so do the *k* values. It was observed that as the GGBS content increased, the permeability coefficient decreased. The permeability coefficient for conventional pervious concrete is 1.8 cm/s. In this study, the lowest value of *k* was noted for 50% GGBS replacement, 10mm aggregate size, and 10% porosity. The *k* values observed in all tests ranged from 1.25 to 1.75 cm/s and are in line with the standard established by ACI 522 R [34]. The results of this study also align with previous research on pervious concrete. The decline in *k* values with increasing GGBS content is due to the increase is density of the mix. Moreover, the rise in C-S-H gel formation with higher GGBS content reduces pores and decreases the thickness of the transition zone in pervious concrete mixes. The water permeability values of a mix are dependent on pore distribution, void size, and aggregate surface roughness. The addition of GGBS significantly affected these properties, leading to a reduction in the water drainage characteristics of pervious concrete. However, the *k* values obtained in this study fell within the desired range, i.e., 0.4 to 1.8 cm/s.

Figure 14 (a) and (b) display the correlations between compressive strength, permeability coefficient, and porosity. There is a positive linear relationship between porosity and permeability, while compressive strength exhibits a negative linear relationship. For both cases, R^2 values were 0.8 and 0.82, which are close to 1, signifying a robust connection between the variables. The negative association between compressive strength and porosity can be attributed to pore roughness. Equation 8 represents the mathematical expression that establishes a linear relationship between compressive strength and permeability.

$$Compressive\ strength = -23.55 \pm 0.97 \times (permeability) \tag{8}$$
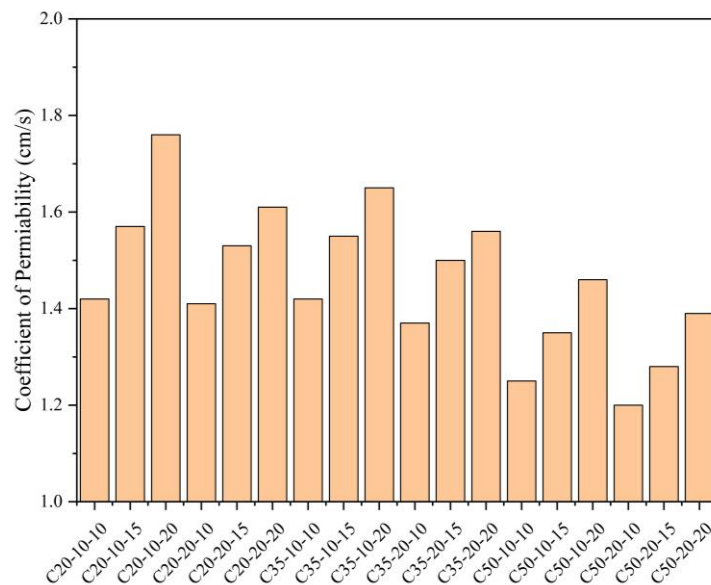
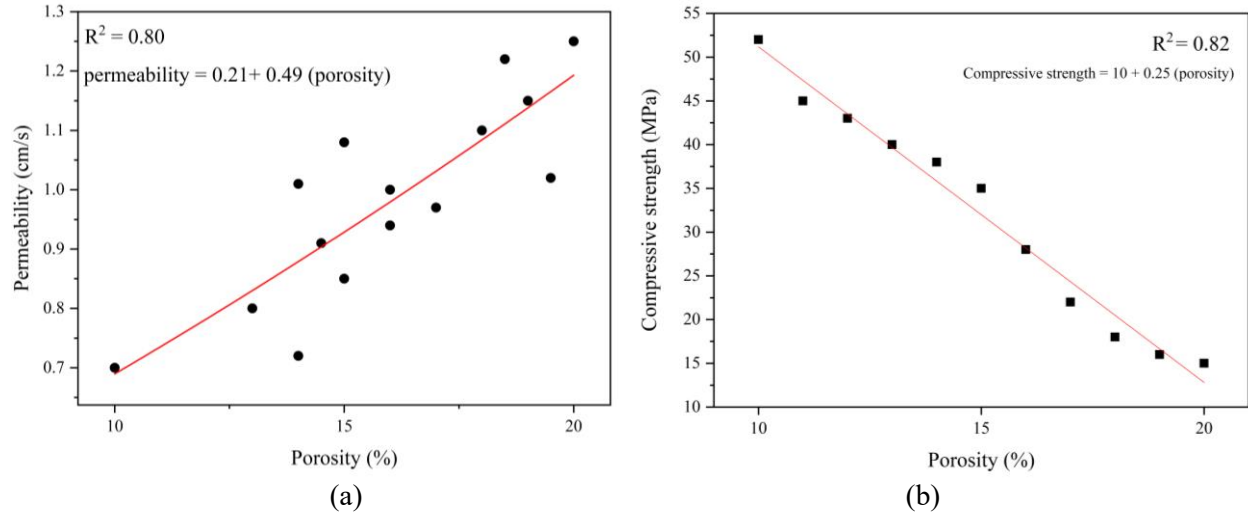**Fig. 13.** Coefficient of permeability measured for various mixtures.

Fig. 14. Comparison of porosity with; (a) permeability, and (b) compressive strength.

4.4. Density

The density of pervious concrete is influenced by the mix's porosity. Cylinders with a height of 200 mm and a diameter of 100 mm were tested for 7-day and 28-day curing periods at various GGBS proportions. The average value of three specimens for each specific proportion was calculated, ranging from 1289 to 1974 kg/m^3. This falls within the suitable range, as pervious concrete pavement density values reported in various studies are estimated to be between 1500 and 2100 kg/m^3 [34]. The main factors contributing to density variation in the mixes were identified as the low-density GGBS and the diverse composition of the supplementary cementitious material.

4.5. Water absorption

Table 4 presents the water absorption values for pervious concrete mixes with varying GGBS proportions, particle sizes, and porosities. In comparison to conventional pervious concrete mixes, water absorption values were found to decrease with extended curing time and increased GGBS content. Water absorption primarily relies on surface phenomena and is indicative of the porous nature of PCP. At a 50% GGBS replacement level, the minimum water absorption value after 7 days of curing is 3.1%, while after 28 days, it is 3.2%. Since GGBS is amorphous and exhibits slow reactivity during cement hydration, a reduction in water absorption values was observed due to its pozzolanic effect. As a result, water absorption values decline as GGBS concentration increases.

Table 4
Water absorption of pervious concrete using different proportions of GGBs.

Pervious concrete mix	Water absorption (%)	
	7-days	28-days
PC-0	6.7	6.5
PC-20	4.5	4.3
PC-35	3.8	3.7
PC-50	3.2	3.1

4.6. Comparison of pervious concrete mixes

A correlation analysis was conducted to examine the relationships between mixes with varying GGBS content, aggregate sizes, and porosity. In this context, GGBS replacement percentage, aggregate sizes, and porosity serve as independent variables. Correlation analysis assesses the interdependence of these independent variables on strength and permeability properties. The present study involves three dependent variables: porosity, strength, and permeability.

The correlation coefficients (r) from Table 5 were plotted against each variable, and most values were found to be larger than 0.5. This indicates that there is a considerable relationship between the dependent and independent variables. The association between porosity and strength is the smallest (-0.25), whereas the relationship between permeability and porosity is the highest (0.91). It may be inferred that using GGBS as a partial replacement for cement results in significant changes in strength and permeability. It is essential to ascertain the most optimal parameter in relation to its strength and permeability. Initially, the study involves development of regression model using multiple linear regression analysis. If any non-linearity exists between the variables, modeling using the ANN technique can reveal the most suitable model.

4.7. MLR and ANN model

The training process encompassed 75% of the available data, and the model for the prediction of compressive strength and permeability is obtained. The model obtains an RMSE values of 0.1312 and 0.1265 for the prediction of compressive strength and permeability respectively. Similarly, the MAPE values are 1.265 and 1.429. Thus, the developed model predicts the compressive strength and permeability with a reasonable accuracy. Likewise, the testing and validation results exhibited diminished RMSE, MAPE, and R^2 values that are close to one. The results of ANN models are shown in Table 6.

On the contrary, the MLR model demonstrated RMSE values of 7.56 and 6.54, as well as MAPE values of 11.56 and 10.54, respectively, for the predictions of compressive strength and permeability. These values are illustrated in Figure 15. The obtained results for compressive strength align with the findings reported by [38] and [39]. However, the existing literature lacks research on the estimation of water permeability in pervious concretes containing GGBS. The accuracy of the ANN model is based on RMSE, MAPE, and R^2 values. The MLR analysis is presented in Equations 11 and 12.

$$f_c = 0.86 \times (\text{aggregate size}) + 1.45 \times (\text{GGBS \%}) - 0.71 \times (\text{porosity}) - 2.56 \qquad (11)$$

$$P = 0.89 \times (\text{aggregate size}) - 1.85 \times (\text{GGBS \%}) + 0.81 \times (\text{porosity}) - 0.62 \qquad (12)$$

Where, f_c is the compressive strength of PC in *MPa*, and *P* is coefficient of permeability in *cm/s*.

Table 5
Correlation between dependent and independent variables.

"R"		Compressive Strength (*MPa*)	Coefficient of Permeability (*cm/s*)	GGBS replacement (%)			Nominal aggregate size (mm)		Porosity (%)		
				20	35	50	10	20	10	15	20
Compressive Strength (*MPa*)		1									
Coefficient of Permeability (*cm/s*)		-0.76	1								
GGBS (%)	20	0.56	-0.68	1							
	35	0.65	-0.53	0.76	1						
	50	0.52	-0.63	0.68	0.72	1					
Aggregate size (mm)	10	0.61	-0.63	0.82	0.83	0.85	1				
	20	0.72	-0.52	0.80	0.86	0.87	0.89	1			
Porosity (%)	10	-0.51	0.86	0.65	0.68	0.71	0.57	0.62	1		
	15	-0.42	0.89	0.57	0.62	0.67	0.55	0.58	0.82	1	
	20	-0.25	0.91	0.52	0.58	0.62	0.48	0.55	0.83	0.85	1

Table 6
Statistics of the ANN model.

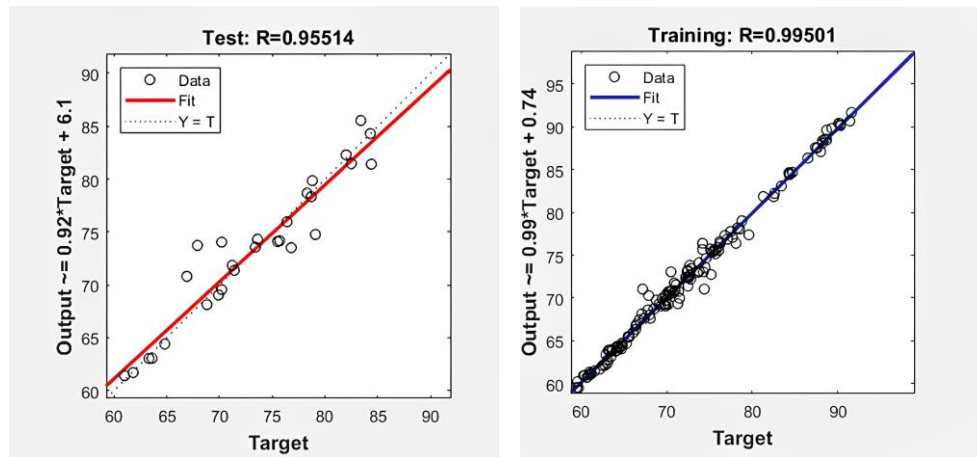| Model Type	Model Training			Model Testing			Model Validation		
	R^2	Root mean square error	Mean absolute percentage error	R^2	Root mean square error	Mean absolute percentage error	R^2	Root mean square error	Mean absolute percentage error
ANN₁	0.99	0.13	1.26	0.99	0.15	1.33	0.99	0.15	1.42
ANN₂	0.99	0.12	1.42	0.99	0.14	1.68	0.99	0.14	1.63

Fig. 15. Scatter plots for training and evaluating an ANN model.

4.8. Sensitivity analysis

Sensitivity analysis was employed in this study to determine the relative significance of independent variables in relation to the dependent variable. The Garson equation [40] was utilized for conducting the sensitivity analysis. Standard deviation calculations were performed for every input parameter, and the deviations from their mean were utilised to evaluate the corresponding changes in the strength and permiability. The present study adopts the variability of output for each input as a sensitivity method, where the variability is quantified in terms of standard deviation. The findings, as depicted in Figure 16, reveal that GGBS and cement exert a more pronounced impact on strength, while perviousness positively correlates with penetrability.

In conclusion, this study highlights the importance of conducting a thorough assessment of ANN compared to traditional models, as there are numerous arbitrary decisions involved in developing an ANN model, including the choice of standard error measures. Limitations of the ANN model includes the use of validation data during training, random input selection, network structure, and inadequate preprocessing of model inputs. Future advancements will contribute to the development of objective guidelines for building ANN models and the creation of standardized metrics to evaluate the performance of these models.
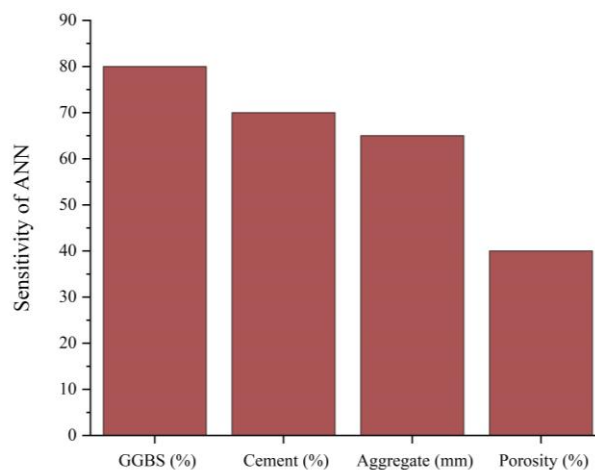

Fig. 16. Sensitivity analysis results of ANN model

5. Conclusions

The primary goal of this study is to evaluate the efficacy and practicality of using GGBS as a partial cement replacement, along with variations in aggregate size and porosity. Strength, permeability, and microstructural properties were analyzed, and predictive models were developed. The subsequent primary deductions were formulated in light of the results obtained from the conducted experimentation:

- Incorporating GGBS in PCP as a partial cement replacement significantly improves compressive and flexural strength. A 35% cement replacement with GGBS results in maximum strength levels of 28% and 20% higher than conventional mix properties. This is due to the strong pozzolanic reaction of GGBS, leading to the formation of calcium silicate hydrate (C-S-H) gel.

- SEM micrograph analysis revealed a denser microstructure in mixes with increasing GGBS levels from 20 to 50%. The C-S-H gel appeared stronger at 35% GGBS replacement than at 50%, suggesting that 35% is the optimum GGBS replacement level in pervious concrete.

- Pervious concrete with GGBS exhibited a permeability coefficient ranging from 1.25 to 1.75 cm/s, significantly lower than conventional pervious concrete. Nonetheless, the permeability values were within acceptable limits for drainage properties. The increase in mix density, reduction in pore size, and thinner transition zone with increasing GGBS content can be attributed to enhanced C-S-H gel formation.

- The density of the pervious concrete samples fell within the acceptable range of 1500 to 2100 kg/m^3.

- Pervious concrete's permeability was assessed using the water absorption test, and lower values indicate higher compressive strength. Among all mixes, the 50% GGBS replacement resulted in the lowest water absorption value of 3.1% due to its amorphous nature and slow reactivity during cement hydration.

- Finally, ANN models containing greater R^2 results and lesser mean-squared errors surpassed MLR in predicting the strength and perviousness of porous concrete. The ANN model's accuracy could be further enhanced by incorporating additional variables, with the changes in the water-cement content proportions or the inclusion of fiber particles.

- The development and validation of ANN models in this study provide an alternative analytical tool for predicting the strength and porousness properties of porous concrete through GGBS content. These models can be used by engineers and construction professionals to optimize the design of pervious concrete mixes and structures, potentially reducing the need for extensive experimental testing.

- This study's findings can serve as a foundation for future research on pervious concrete incorporating GGBS or other supplementary cementitious materials. Researchers can further investigate the long-term performance, durability, and environmental impact of such materials, as well as explore other factors that may influence their properties, such as fiber reinforcement or alternative aggregate sources.

While the study provides valuable insights into the effects of GGBS on pervious concrete's strength and permeability, there are several limitations that should be considered:

- Mix proportions: The study focused on specific mix proportions and GGBS replacement levels. The results may not be directly applicable to pervious concrete mixes with different mix proportions or GGBS content outside the tested range.
- Limited parameters: The study examined the impact of GGBS content, aggregate size, and porosity. Additional factors, such as water-cement ratio, admixtures, or fiber reinforcement, could also affect the performance of pervious concrete but were not considered in this investigation.
- Generalizability: The findings might not be directly applicable to all types of pervious concrete or regional materials, as the study utilized a specific type of GGBS and aggregates. Further research using different materials and sources could be necessary to confirm the results.
- ANN model limitations: The ANN models developed in this study are based on the data collected from the experiments. While these models outperformed the traditional MLR model, the accuracy and predictive capabilities of the ANN models could be influenced by factors such as network structure, input selection, and data preprocessing. Additionally, the ANN models may not account for non-linear relationships between variables, which could affect their performance in predicting strength and permeability.
- Long-term performance: The study focused on the compressive strength and permeability of pervious concrete at specific curing times (7 and 28 days). The long-term performance of pervious concrete with GGBS under different environmental conditions, such as freeze-thaw cycles or exposure to chemical agents, was not investigated.
- Experimental setup: The study's conclusions are based on laboratory tests, which may not fully replicate real-world conditions. Field trials of pervious concrete containing GGBS would be necessary to validate the findings under actual service conditions.

Funding

Conflicts of interest

The authors declare no conflict of interest.

Authors contribution statement

Boddu Sudhir Kumar, Kakara Srikanth: Conceptualization; Boddu Sudhir Kumar, Tammali Eeshwar: Data analysis; Kakara Srikanth: Formal analysis; Boddu Sudhir Kumar, Kakara Srikanth: Investigation; Boddu Sudhir Kumar, Kakara Srikanth: Methodology; Boddu Sudhir Kumar: Project administration; Boddu Sudhir Kumar: Resources; Boddu Sudhir Kumar: Supervision; Boddu Sudhir Kumar, Kakara Srikanth: Validation; Boddu Sudhir Kumar, Kakara Srikanth: Visualization; Boddu Sudhir Kumar, Kakara Srikanth: Roles/Writing – original draft; Boddu Sudhir Kumar, Kakara Srikanth, Tammali Eeshwar: Writing – review & editing.

References

[1]   Ahmad W, Ahmad A, Ostrowski KA, Aslam F, Joyklad P. A scientometric review of waste material utilization in concrete for sustainable construction. Case Stud Constr Mater 2021;15:e00683. https://doi.org/10.1016/j.cscm.2021.e00683.

[2]   Sarkar M, Adak D, Tamang A, Chattopadhyay B, Mandal S. Genetically-enriched microbe-facilitated self-healing concrete – a sustainable material for a new generation of construction technology. RSC Adv 2015;5:105363–71. https://doi.org/10.1039/C5RA20858K.

[3]   Zhong R, Leng Z, Poon C. Research and application of pervious concrete as a sustainable pavement material: A state-of-the-art and state-of-the-practice review. Constr Build Mater 2018;183:544–53. https://doi.org/10.1016/j.conbuildmat.2018.06.131.

[4]   Liew KM, Sojobi AO, Zhang LW. Green concrete: Prospects and challenges. Constr Build Mater 2017;156:1063–95. https://doi.org/10.1016/j.conbuildmat.2017.09.008.

[5]   Elango KS, Gopi R, Saravanakumar R, Rajeshkumar V, Vivek D, Raman SV. Properties of pervious concrete – A state of the art review. Mater Today Proc 2021;45:2422–5. https://doi.org/10.1016/j.matpr.2020.10.839.

[6]   Bonicelli A, Arguelles GM, Pumarejo LGF. Improving Pervious Concrete Pavements for Achieving More Sustainable Urban Roads. Procedia Eng 2016;161:1568–73. https://doi.org/10.1016/j.proeng.2016.08.628.

[7]   Lu J-X, Yan X, He P, Poon CS. Sustainable design of pervious concrete using waste glass and recycled concrete aggregate. J Clean Prod 2019;234:1102–12. https://doi.org/10.1016/j.jclepro.2019.06.260.

[8]   Alireza Joshaghani, Alireza Moazenian, Richard Abubakar Shuaibu. Experimental Study on the Use of Trass as a Supplementary Cementitious Material in Pervious Concrete. J Environ Sci Eng A 2017;6. https://doi.org/10.17265/2162-5298/2017.01.005.

[9]   Adamu M, Ayeni KO, Haruna SI, Ibrahim Mansour YE-H, Haruna S. Durability performance of pervious concrete containing rice husk ash and calcium carbide: A response surface methodology approach. Case Stud Constr Mater 2021;14:e00547. https://doi.org/10.1016/j.cscm.2021.e00547.

[10]   Ahmad J, Martínez-García R, Szelag M, De-Prado-Gil J, Marzouki R, Alqurashi M, et al. Effects of Steel Fibers (SF) and Ground Granulated Blast Furnace Slag (GGBS) on Recycled Aggregate Concrete. Materials (Basel) 2021;14:7497. https://doi.org/10.3390/ma14247497.

[11]   Sun Z, Lin X, Vollpracht A. Pervious concrete made of alkali activated slag and geopolymers. Constr Build Mater 2018;189:797–803. https://doi.org/10.1016/j.conbuildmat.2018.09.067.

[12]   An Q, Pan H, Zhao Q, Du S, Wang D. Strength development and microstructure of recycled gypsum-soda residue-GGBS based geopolymer. Constr Build Mater 2022;331:127312. https://doi.org/10.1016/j.conbuildmat.2022.127312.

[13]   El-Hassan H, Kianmehr P. Pervious concrete pavement incorporating GGBS to alleviate pavement runoff and improve urban sustainability. Road Mater Pavement Des 2018;19:167–81. https://doi.org/10.1080/14680629.2016.1251957.

[14]   Almasaeid HH, Salman DG. Application of Artificial Neural Network to Predict the Properties of Permeable Concrete. Civ Eng Archit 2022;10:2290–305. https://doi.org/10.13189/cea.2022.100605.

[15]   Adewumi AA, Owolabi TO, Alade IO, Olatunji SO. Estimation of physical, mechanical and hydrological properties of permeable concrete using computational intelligence approach. Appl Soft Comput 2016;42:342–50. https://doi.org/10.1016/j.asoc.2016.02.009.

[16]   Shanmuganathan S. Artificial Neural Network Modelling: An Introduction, 2016, p. 1–14. https://doi.org/10.1007/978-3-319-28495-8_1.

[17] Suri RS, Jain AK, Kapoor NR, Kumar A, Arora HC, Kumar K, et al. Air Quality Prediction - A Study Using Neural Network Based Approach. J Soft Comput Civ Eng 2023;7:93–113. https://doi.org/10.22115/scce.2022.352017.1488.

[18] Kapoor NR, Kumar A, Kumar A, Kumar A, Kumar K. Transmission Probability of SARS-CoV-2 in Office Environment Using Artificial Neural Network. IEEE Access 2022;10:121204–29. https://doi.org/10.1109/ACCESS.2022.3222795.

[19] Kapoor NR, Kumar A, Kumar A, Kumar A, Mohammed MA, Kumar K, et al. Machine Learning-Based CO2 Prediction for Office Room: A Pilot Study. Wirel Commun Mob Comput 2022;2022:1–16. https://doi.org/10.1155/2022/9404807.

[20] Wadhawan S, Bassi A, Singh R, Patel M. Prediction of Compressive Strength for Fly Ash-Based Concrete: Critical Comparison of Machine Learning Algorithms. J Soft Comput Civ Eng 2023;7:68–110. https://doi.org/10.22115/scce.2023.353183.1493.

[21] Arora HC, Kumar S, Kontoni D-PN, Kumar A, Sharma M, Kapoor NR, et al. Axial Capacity of FRP-Reinforced Concrete Columns: Computational Intelligence-Based Prognosis for Sustainable Structures. Buildings 2022;12:2137. https://doi.org/10.3390/buildings12122137.

[22] Kumar A, Arora HC, Kapoor NR, Kumar K, Hadzima-Nyarko M, Radu D. Machine learning intelligence to assess the shear capacity of corroded reinforced concrete beams. Sci Rep 2023;13:2857. https://doi.org/10.1038/s41598-023-30037-9.

[23] al-Swaidani AM, Khwies WT. Applicability of Artificial Neural Networks to Predict Mechanical and Permeability Properties of Volcanic Scoria-Based Concrete. Adv Civ Eng 2018;2018:5207962. https://doi.org/10.1155/2018/5207962.

[24] Baykasoglu A, Dereli T, Tanış S. Prediction of cement strength using soft computing techniques. Cem Concr Res 2004;34:2083–90. https://doi.org/10.1016/j.cemconres.2004.03.028.

[25] Kumar BS, Srikanth K. A study on properties of pervious concrete with high-volume usage of supplementary cementitious materials as substitutes for cement. Asian J Civ Eng 2023. https://doi.org/10.1007/s42107-023-00619-z.

[26] Golafshani EM, Behnood A. Predicting the mechanical properties of sustainable concrete containing waste foundry sand using multi-objective ANN approach. Constr Build Mater 2021;291:123314. https://doi.org/https://doi.org/10.1016/j.conbuildmat.2021.123314.

[27] Behnood A, Golafshani EM. Predicting the compressive strength of silica fume concrete using hybrid artificial neural network with multi-objective grey wolves. J Clean Prod 2018;202:54–64. https://doi.org/https://doi.org/10.1016/j.jclepro.2018.08.065.

[28] Kumar BS, Chowdary V. Use of artificial neural networks to assess train horn noise at a railway level crossing in India. Environ Monit Assess 2023;195:426. https://doi.org/10.1007/s10661-023-11021-2.

[29] Debnath M, Sarma AK, Mahanta C. Development of ANN Model for Simulation of the Runoff as Affected by Climatic Factors on the Jamuna River, Assam, India. Water Energy Manag. India, Cham: Springer International Publishing; 2021, p. 127–39. https://doi.org/10.1007/978-3-030-66683-5_6.

[30] Bureau of Indian Standards (BIS). Method of physical tests for hydraulic cement: Determination of fineness by dry sieving. IS 4031 Part 1, New Delhi 1996:Reaffirmed in 2005.

[31] IRC 44. Guidelines for Cement Concrete Mix Design for Pavements. Indian Roads Congr 2017:1–60.

[32] IS 516. Method of Tests for Strength of Concrete. Bur Indian Stand 1959:1–30.

[33] IS 5816-1999. Indian standard Splitting tensile strength of concrete- method of test. Bur Indian Stand 1999:1–14.

[34] ACI Committee 522: 522R-10: Report on Pervious Concrete. 2010.

[35] Siddique R, Aggarwal Y, Aggarwal P, Kadri E-H, Bennacer R. Strength, durability, and micro-structural properties of concrete made with used-foundry sand (UFS). Constr Build Mater 2011;25:1916–25. https://doi.org/10.1016/j.conbuildmat.2010.11.065.

[36] Wild S, Khatib JM, Jones A. Relative strength, pozzolanic activity and cement hydration in superplasticised metakaolin concrete. Cem Concr Res 1996;26:1537–44. https://doi.org/10.1016/0008-8846(96)00148-2.

[37] Zhong R, Wille K. Compression response of normal and high strength pervious concrete. Constr Build Mater 2016;109:177–87. https://doi.org/10.1016/j.conbuildmat.2016.01.051.

[38] Chithra S, Kumar SRRS, Chinnaraju K, Alfin Ashmita F. A comparative study on the compressive strength prediction models for High Performance Concrete containing nano silica and copper slag using regression analysis and Artificial Neural Networks. Constr Build Mater 2016;114:528–35. https://doi.org/10.1016/j.conbuildmat.2016.03.214.

[39] García Á, Anjos O, Iglesias C, Pereira H, Martínez J, Taboada J. Prediction of mechanical strength of cork under compression using machine learning techniques. Mater Des 2015;82:304–11. https://doi.org/10.1016/j.matdes.2015.03.038.

[40] Dibakor Boruah, Pintu Kumar Thakur, Dipal Baruah. Artificial Neural Network based Modelling of Internal Combustion Engine Performance. Int J Eng Res 2016;V5. https://doi.org/10.17577/IJERTV5IS030924.